

Modifications of boronic ester pro-chelators triggered by hydrogen peroxide tune reactivity to inhibit metal-promoted oxidative stress†

Louise K. Charkoudian, David M. Pham, Ashley M. Kwon, Abbey D. Vangeloff and Katherine J. Franz*

Supporting Information

* Department of Chemistry, Duke University, Durham, NC 27708-0346 USA. Fax: +1 919 660 1605; Tel: +1 919 660 1541; E-mail: katherine.franz@duke.edu

X-ray Data Collection and Structure Solution Refinement.

Colorless needles of the chelators {SBH(*m*-OMe), SBH(*m*-OEt), SBH(OMe)₃} and pro-chelators {BSBH(*m*-OMe), [SBH(*m*-OEt)]₂•H₂O} were crystallized by slow evaporation of ethanol. Black needles of [Fe(SBH(OMe)₃)₂]NO₃•pentanes were crystallized in a 6 mm glass tube by slowly diffusing pentanes into a saturated solution of [Fe(SBH(OMe)₃)₂]NO₃ dissolved in chlorobenzene. The crystals were mounted on the tip of a glass fiber and held in place by epoxy glue. Data were collected at 298 K for SBH(*m*-OEt), BSBH(*m*-OMe), SBH(*m*-OEt), and [Fe(SBH(OMe)₃)₂]NO₃•pentanes and at 173 K for the SBH(*m*-OMe), and SBH(OMe)₃.

All diffraction experiments were performed on a Bruker Kappa Apex II CCD diffractometer equipped with a graphite monochromator and a Mo K α fine-focus sealed tube ($\lambda = 0.71073 \text{ \AA}$) operated at 1.75 kW power (50 kV, 35 mA). The detector was placed at a distance of 5.010 cm from the crystal. Each data set was collected with a total of 1548 frames and a scan width of 0.5°. Exposure times for each experiment were dependent on diffraction intensity of each sample. The frames were integrated with the Bruker SAINT v7.12A software package using a narrow-frame integration algorithm. Empirical absorption corrections were applied using SADABS v2.10 and the structure was checked for higher symmetry with PLATON v1.07. The structures were solved by direct methods with refinement by full-matrix least-squares based on F^2 using the Bruker SHELXTL Software Package. All non-hydrogen atoms were refined anisotropically, with the exception of disordered solvent molecules and minor disordered components. Hydrogen atoms of sp^2 hybridized carbons and nitrogens were located directly from the difference Fourier maps; all others were calculated.

Anterior components of the pinacolboronate functionality tend to show higher thermal motion than the rest of the molecules that they are attached to, because the fluxional five-membered ring can take on multiple conformations. In the [SBH(*m*-OEt)]₂•H₂O structure, there are two unique SBH(*m*-OEt) moieties in the asymmetric unit, but only one of the two contained multiple distinguishable conformations of the pinacolboronate group.

One of the two SBH(OMe)₃ ligands in the [Fe(SBH(OMe)₃)₂]NO₃•pentanes structure contains two orientations for the trimethoxyphenyl group. The minor components were initially determined from the difference map and then constraint to a rigid group model for the refinements. Refinement for the occupancies of the two orientations was refined to be 87.5% and 12.5%.

Figure S1-6 shows the fully labeled structure. A full list of atom coordinates and anisotropic displacement parameters can be found in cif format in a separate file of Supplemental Information.

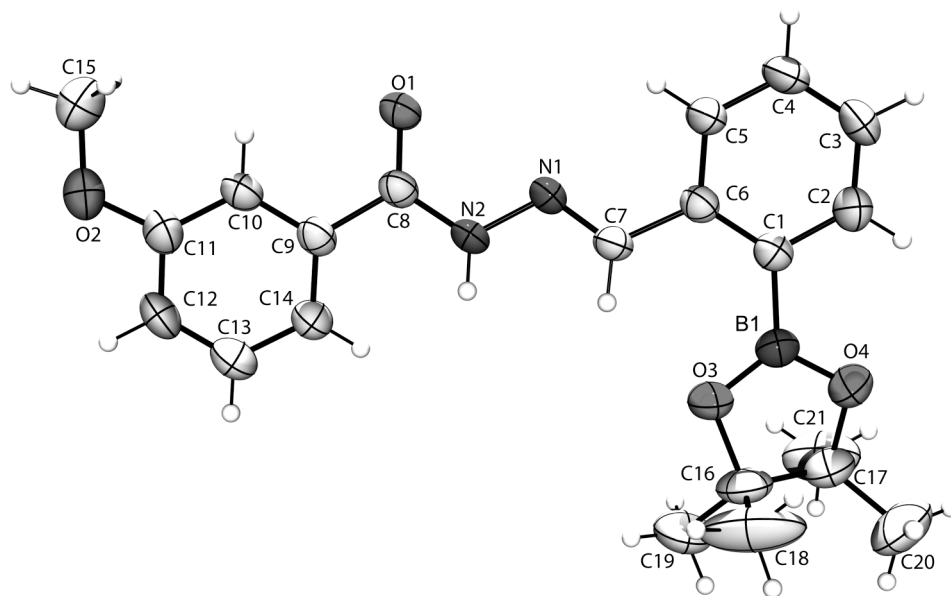


Fig. S1 ORTEP structural diagrams showing 50% probability ellipsoids and full atom numbering schemes for the pro-chelator BSBH(*m*-OMe).

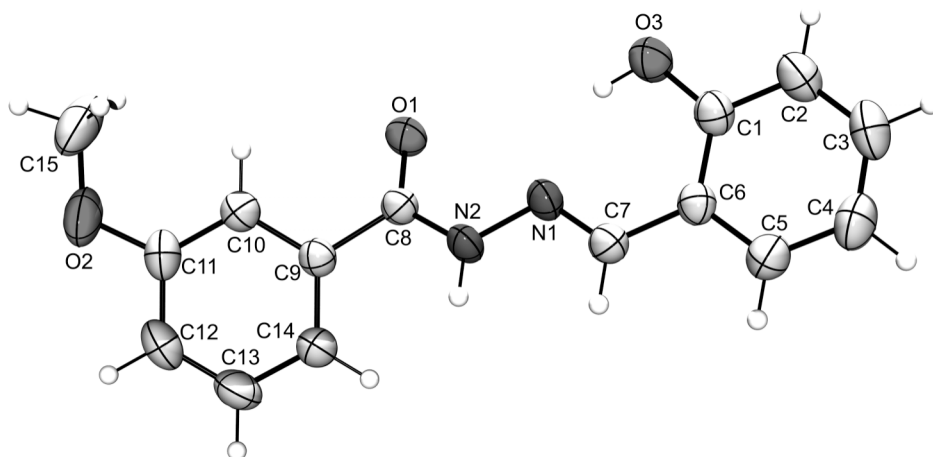


Fig. S2 ORTEP structural diagrams showing 50% probability ellipsoids and full atom numbering schemes for the chelator SBH(*m*-OMe).

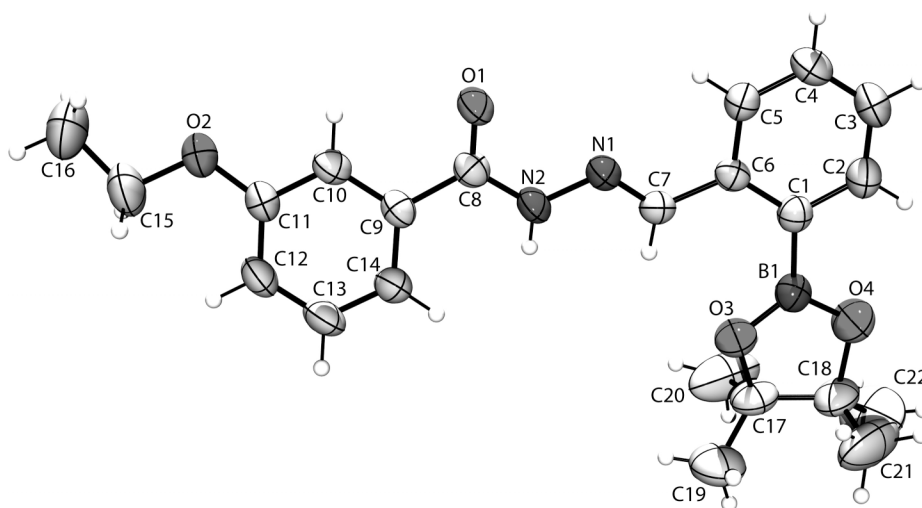


Fig. S3 ORTEP structural diagrams showing 50% probability ellipsoids and full atom numbering schemes for the pro-chelator SBH(*m*-OEt).

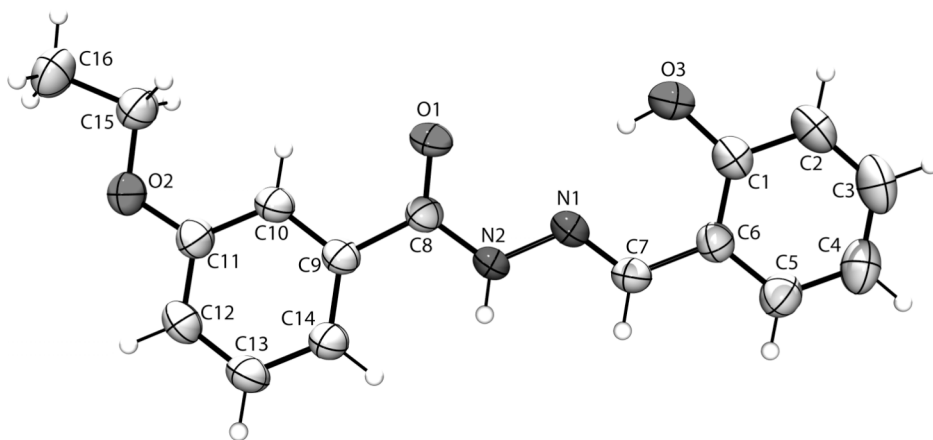


Fig. S4 ORTEP structural diagrams showing 50% probability ellipsoids and full atom numbering schemes for the chelator SBH(*m*-OEt).

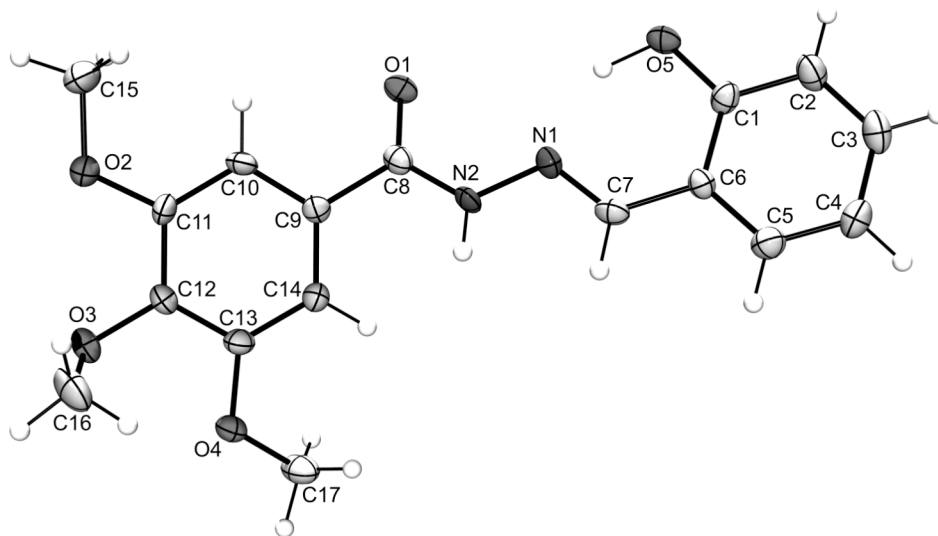


Fig. S5 ORTEP structural diagrams showing 50% probability ellipsoids and full atom numbering schemes for the chelator SBH(OMe)₃.

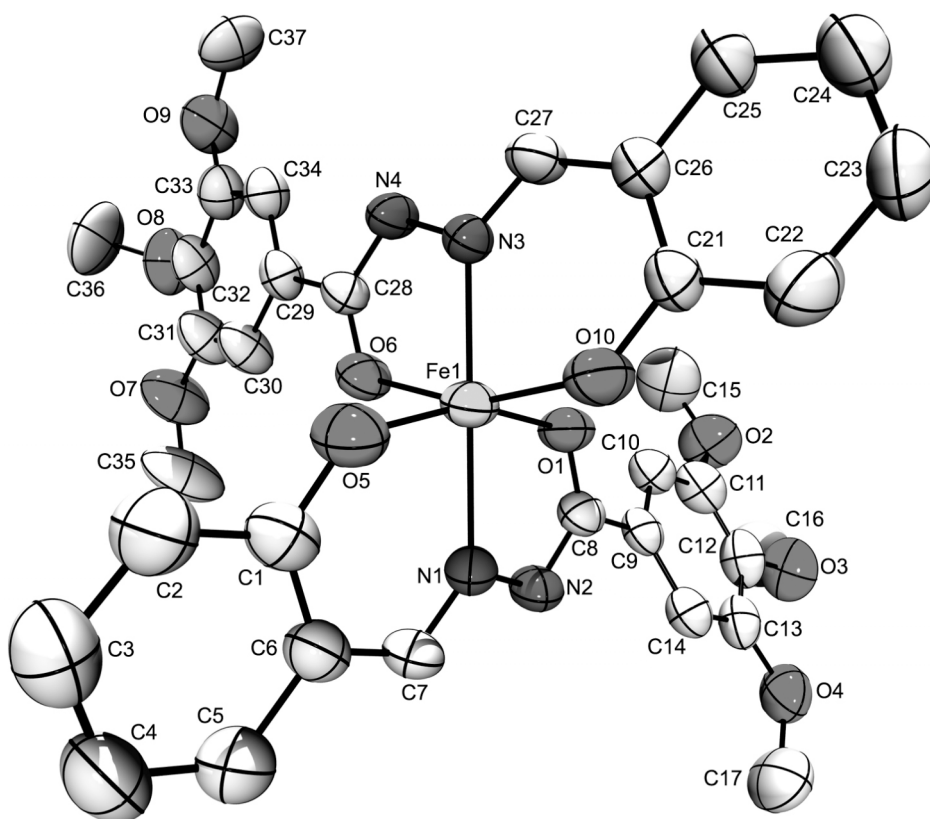


Fig. S6 ORTEP structural diagrams showing 50% probability ellipsoids and full atom numbering schemes for the [Fe(SBH(OMe)₃)₂]⁺ complex.

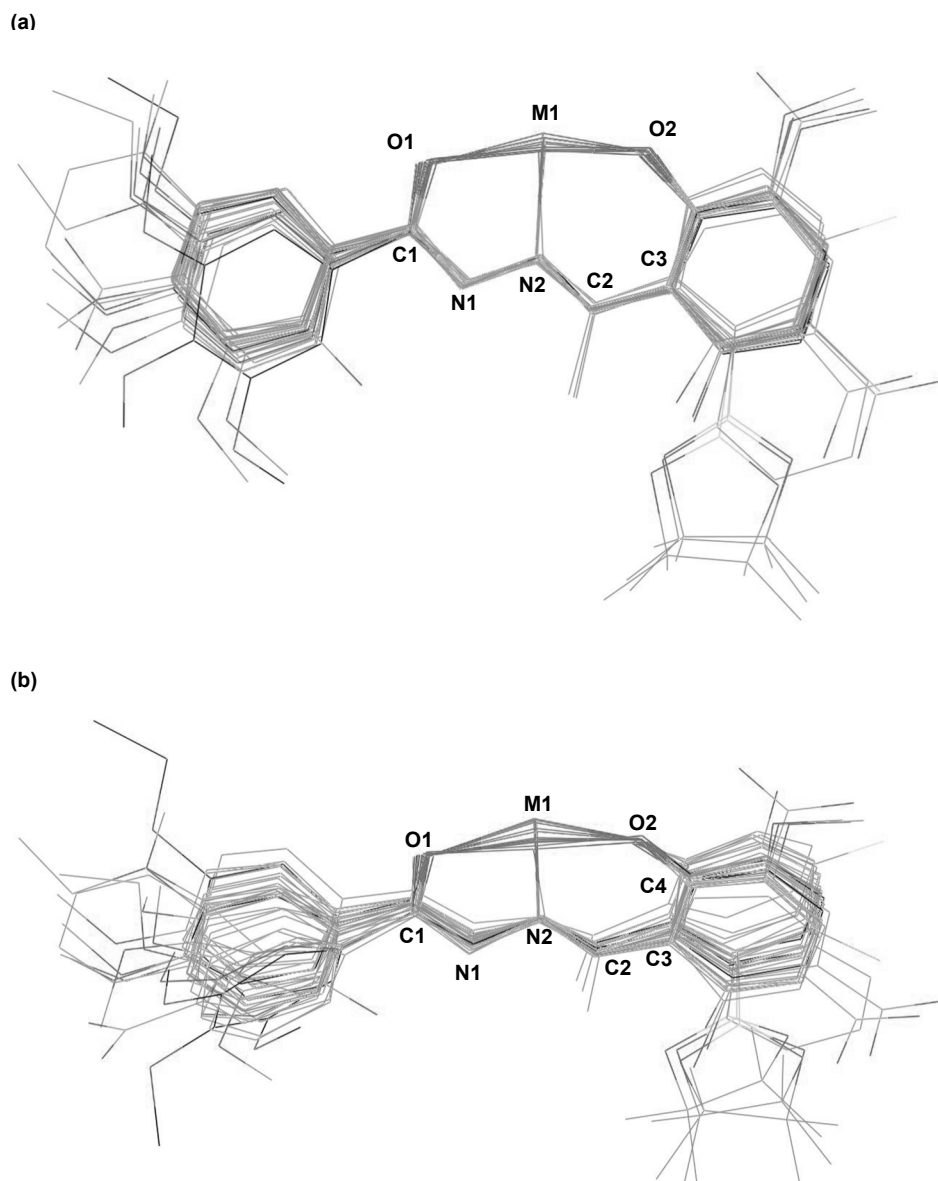


Fig. S7 A composite of 33 SIH and SBH derivatives, which included 18 free ligands and 15 metal complexes, that resulted from a Cambridge Structure Database search were imported into Mercury 1.4.1, part of the CCDC software package. The positions of the three donor sites {O1, N2, O2} of all structures were projected onto the $[\text{FeCl}_2(\text{MeOH})\text{SBH}]\cdot\text{MeOH}$ structure using the Structure Overlay function in the Mercury software. **(a)** Flattened projection of all the molecules to illustrate the very slight deviations from structure to structure about the center of all the ligands. **(b)** This illustration shows the angled perspective of the projection of all 33 structures to show the relatively conserved core of the ligands and the spatial variations of the flanking functional groups.

Fig S8. ^1H -NMR spectrum of BASIH in deuterated methanol (CD_3OD) at 25°C .

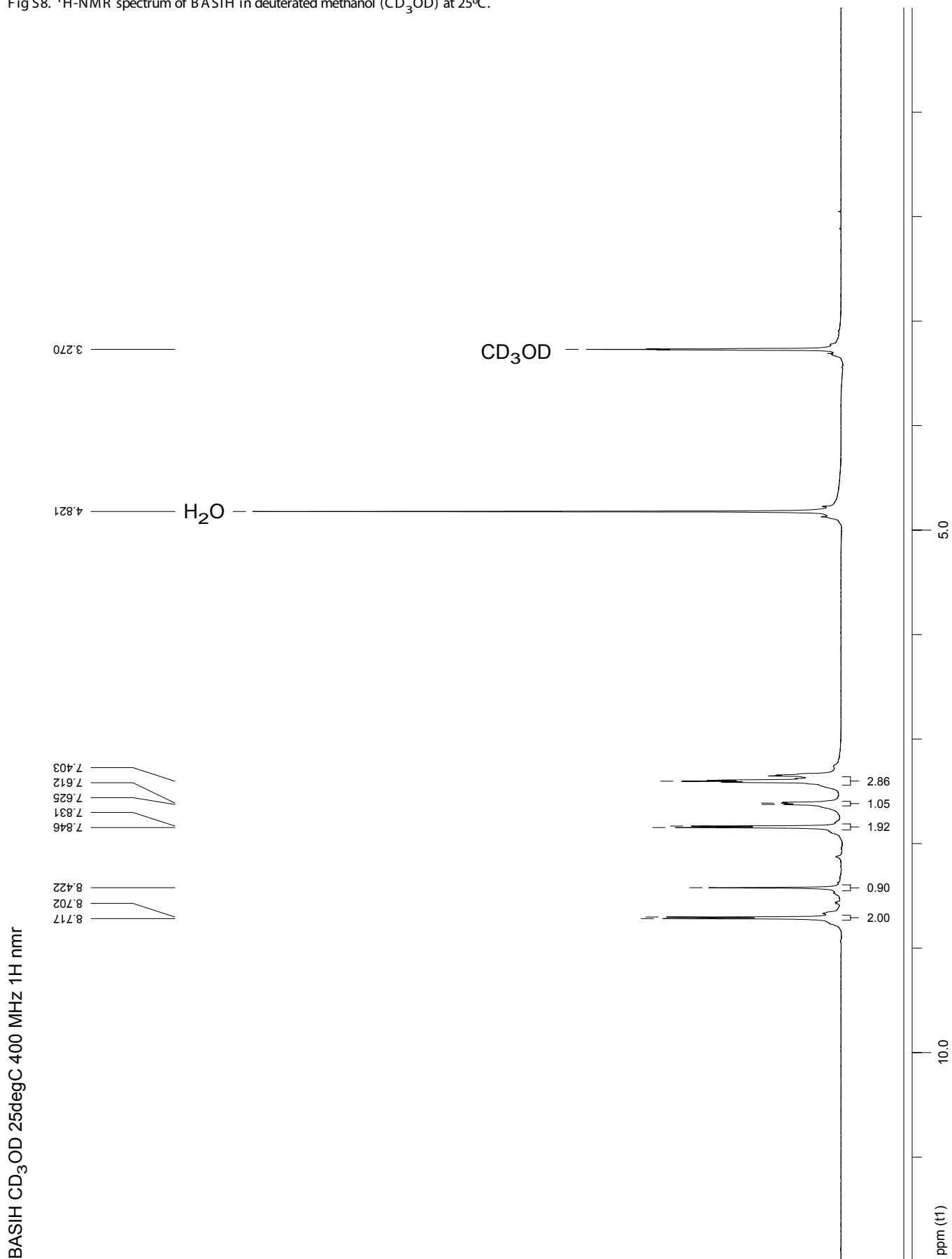


Fig S9. $^1\text{H-NMR}$ spectrum of (p-MeO)BASIH in deuterated methanol (CD_3OD) at 25°C .

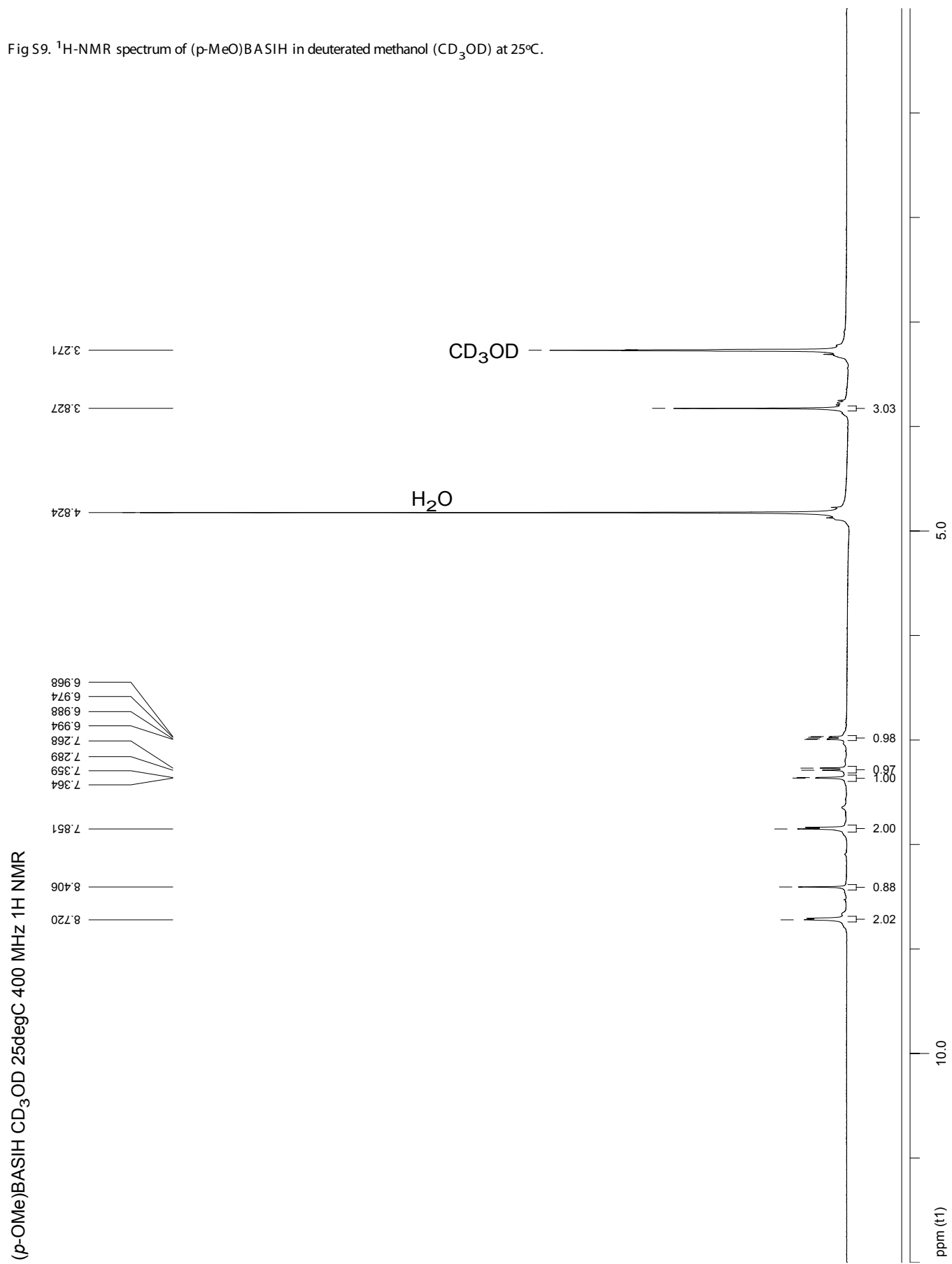


Fig S10. ¹H-NMR spectrum of (p-MeO)SIH in deuterated methanol (CD₃OD) at 25°C. (p-MeO)SIH was generated in the nmr tube with from the reaction of (p-MeO)BASIH with 10 molar equivalents of H₂O₂ (50% aqueous solution) in CD₃OD.

Reaction of (p-Ome)BASIH with 10 eq H₂O₂ to form (p-Ome)SIH. CD₃OD 25degC 400 mHz 1H nmr

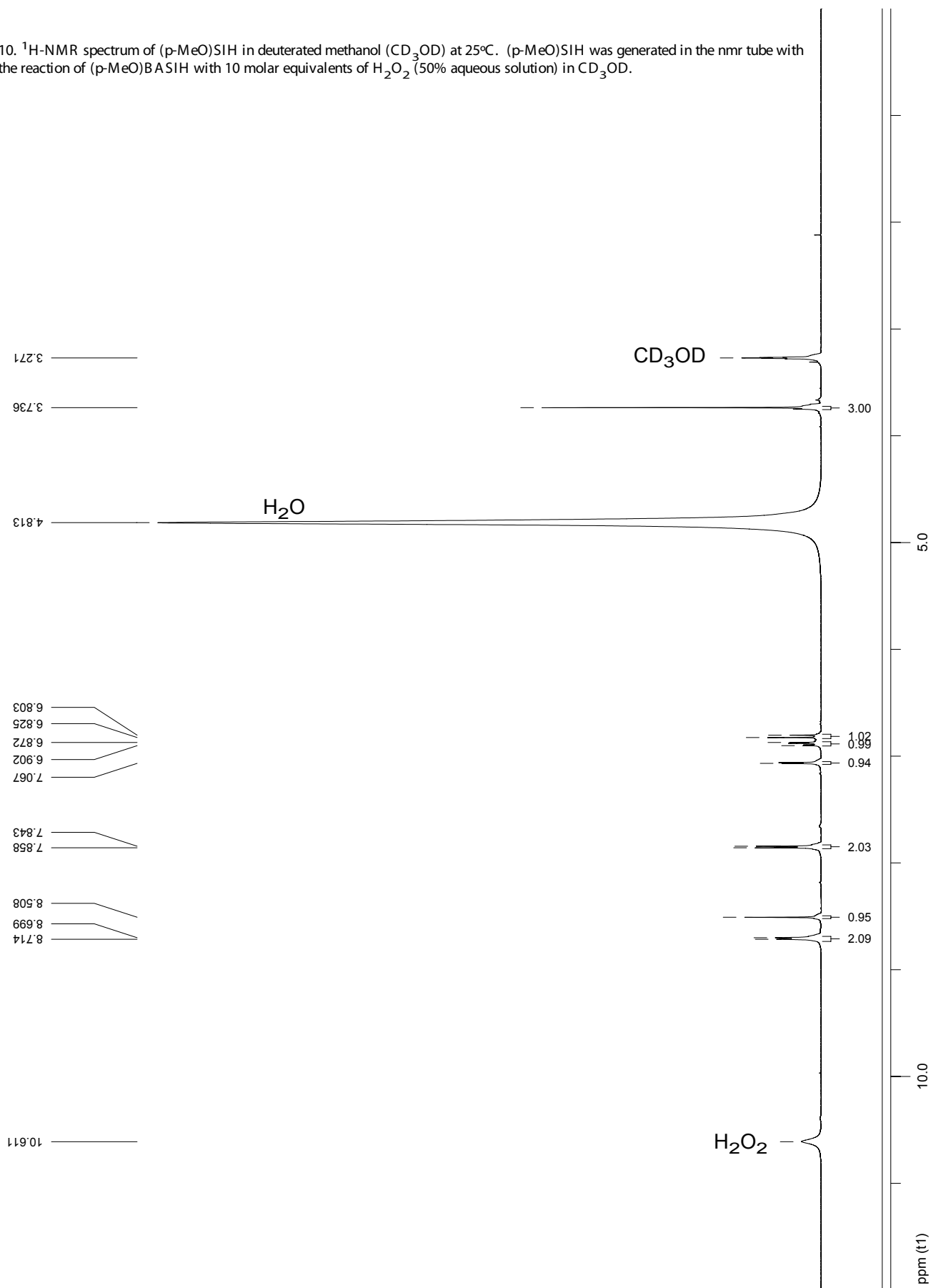


Fig S11. ¹H-NMR spectrum of (m-Cl)BASIH in deuterated methanol (CD₃OD) at 25°C.

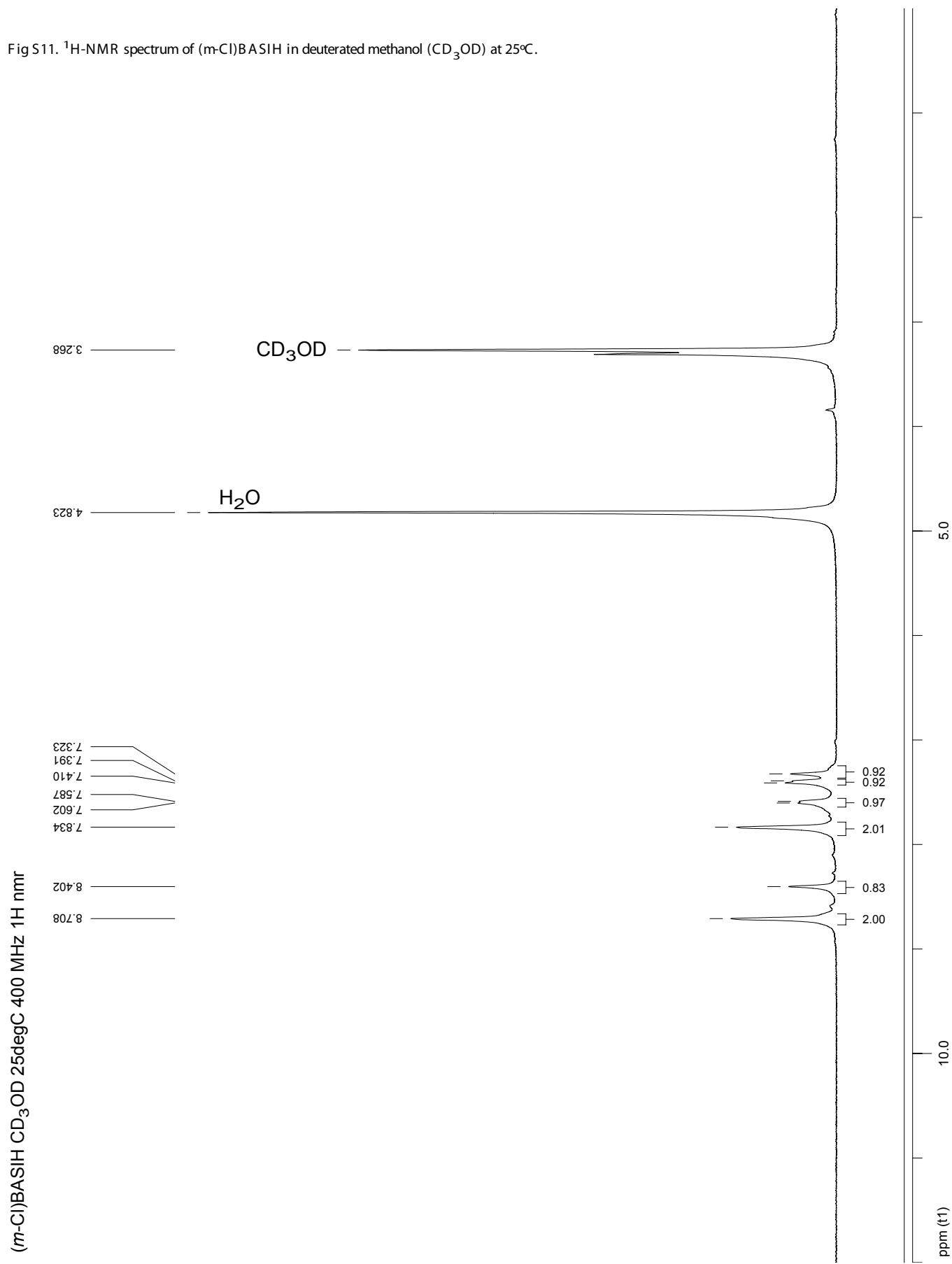


Fig S12. $^1\text{H-NMR}$ spectrum of (*m*-Cl)SIH in deuterated methanol (CD_3OD) at 25°C . (*m*-Cl)SIH was generated in the nmr tube with from the reaction of (*m*-Cl)BASIH with 10 molar equivalents of H_2O_2 (50% aqueous solution) in CD_3OD .

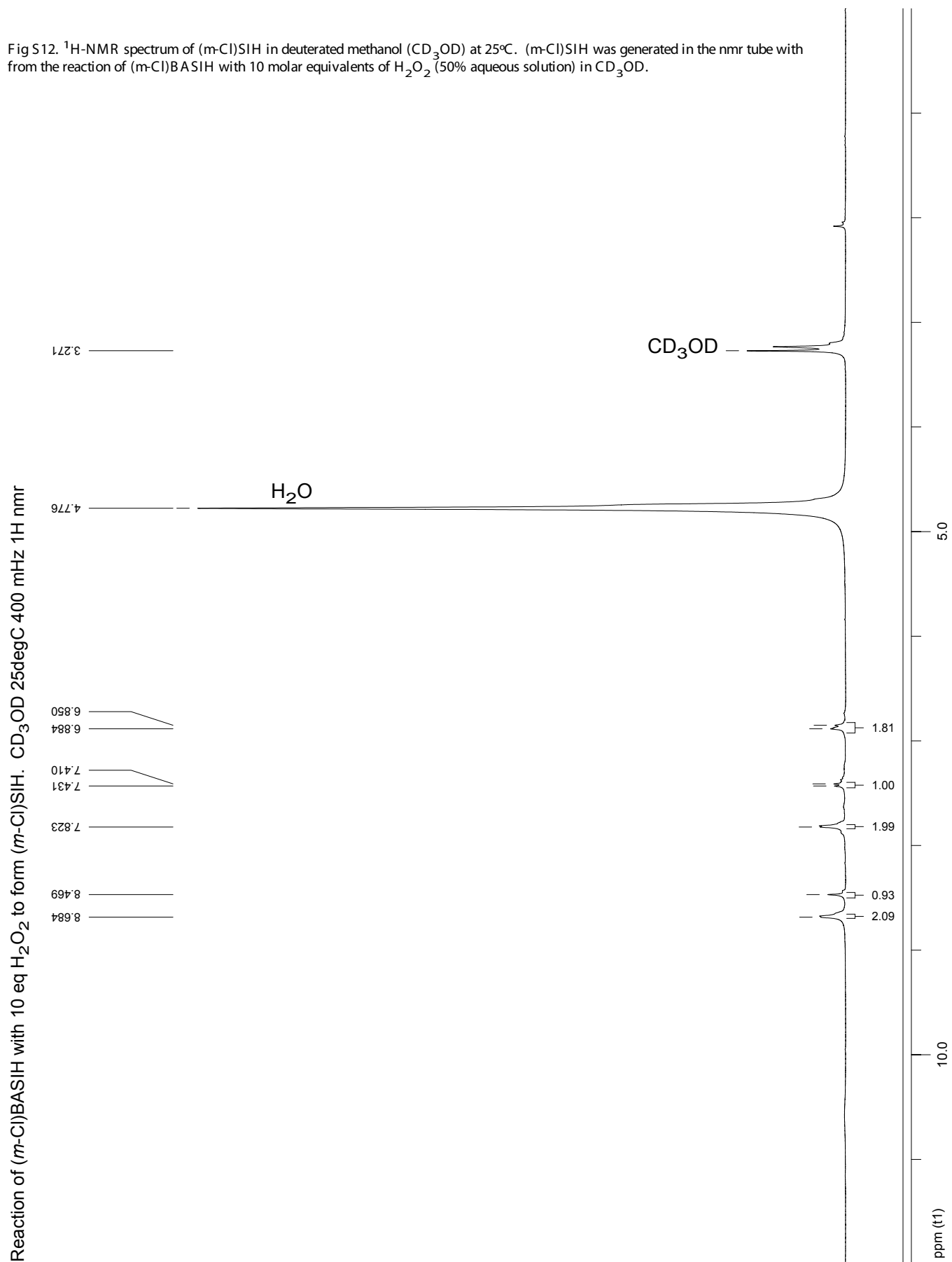


Fig S13. ¹H-NMR spectrum of BIH in deuterated methanol (CD₃OD) at 25°C.

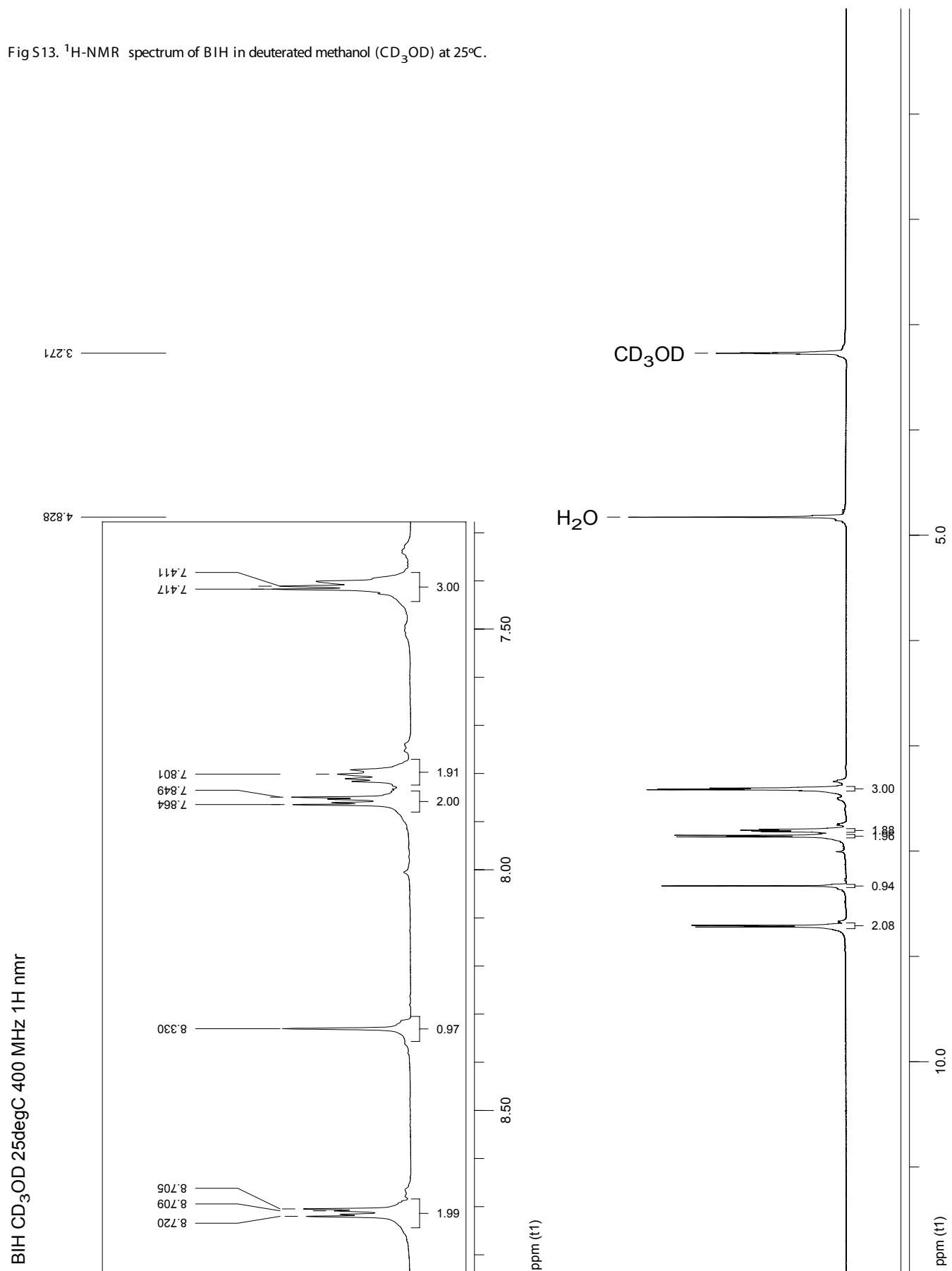


Fig S15. $^1\text{H-NMR}$ spectrum of SBH(*m*-OMe) in deuterated DMSO ($\text{C}_2\text{D}_6\text{SO}$) at 25°C .

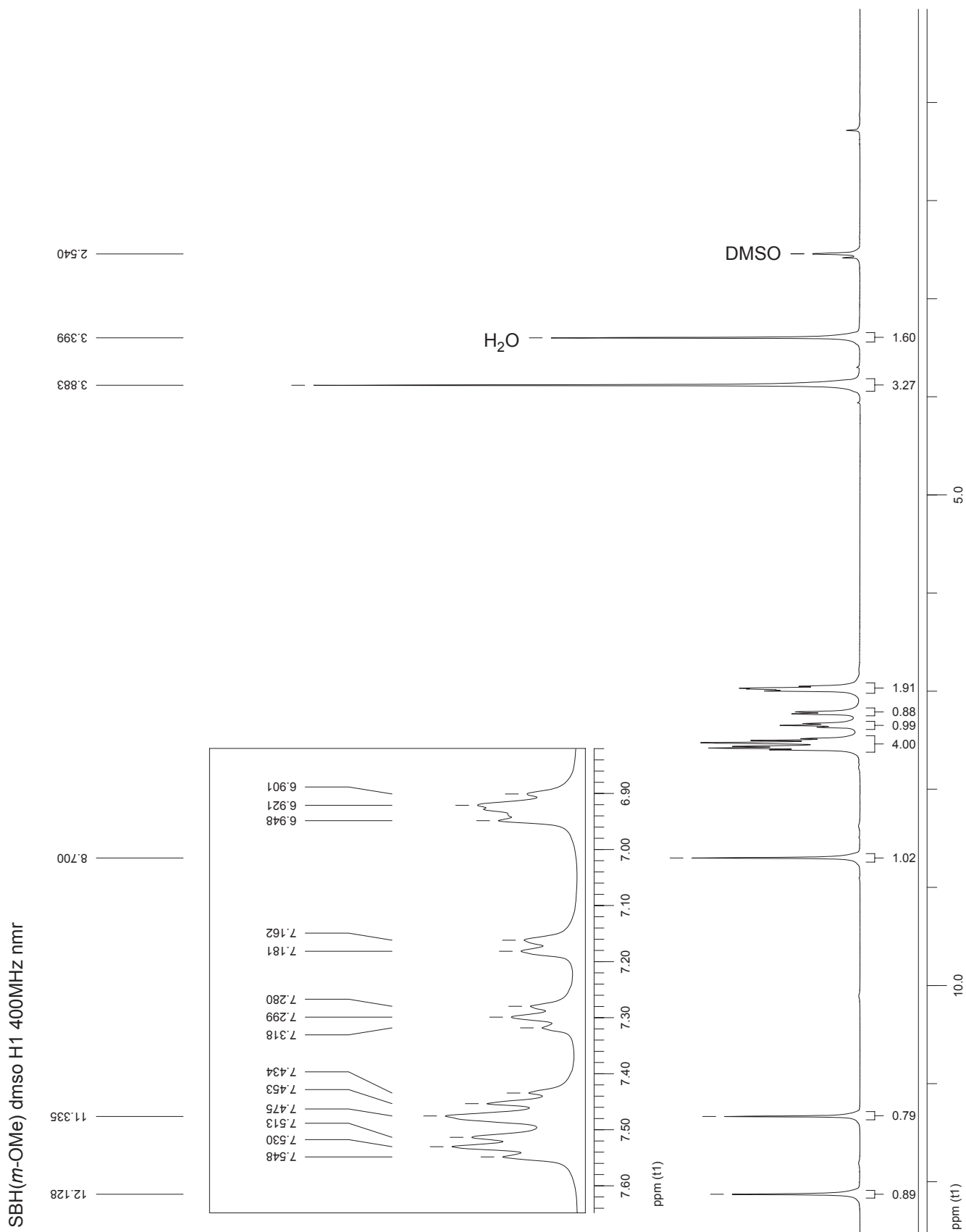


Fig S16. ¹H-NMR spectrum of BSBH(m-OEt) in deuterated DMSO (C₂D₆SO) at 25°C.

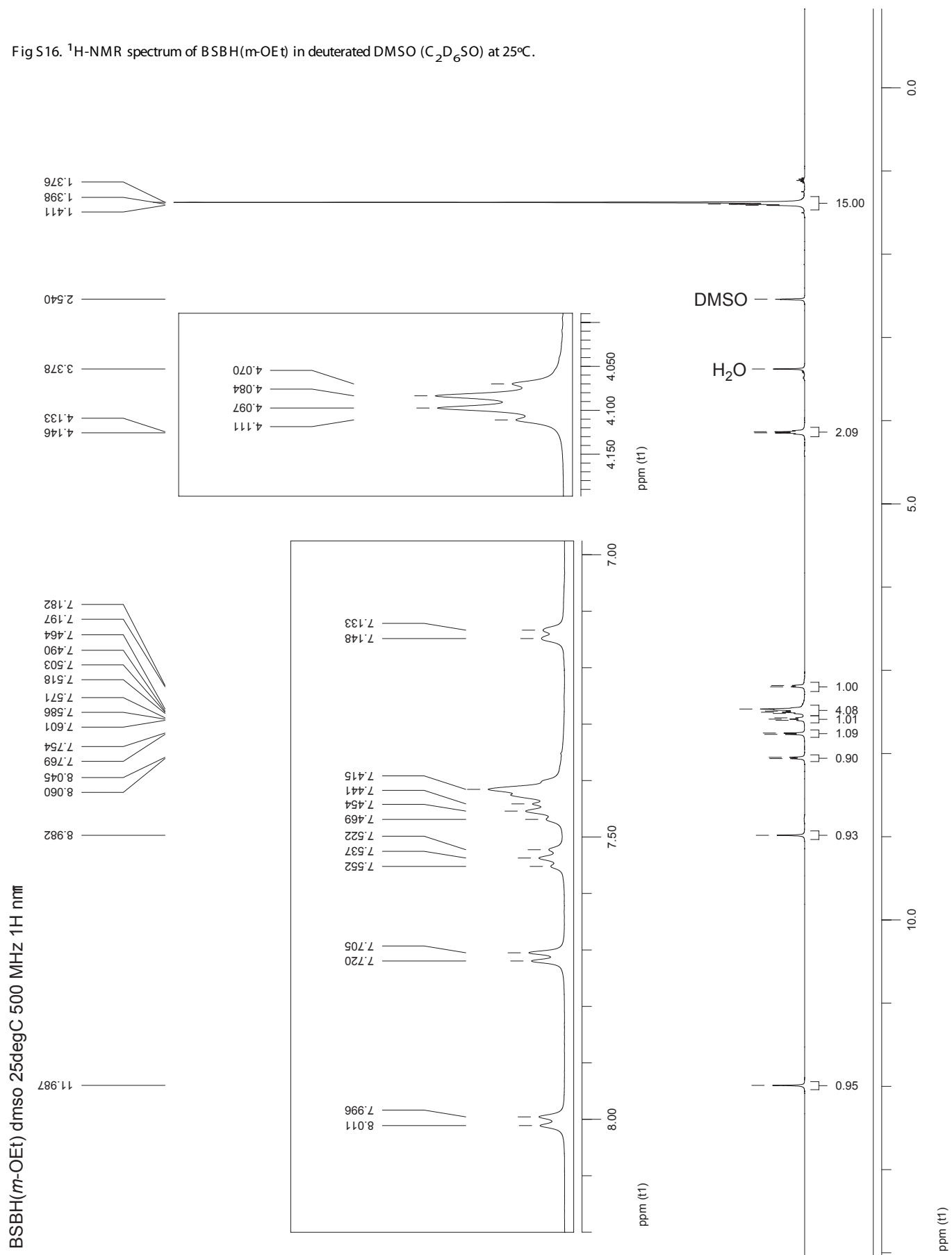


Fig S17. ¹H-NMR spectrum of SBH(*m*-OEt) in deuterated DMSO (C₂D₆SO) at 25°C.

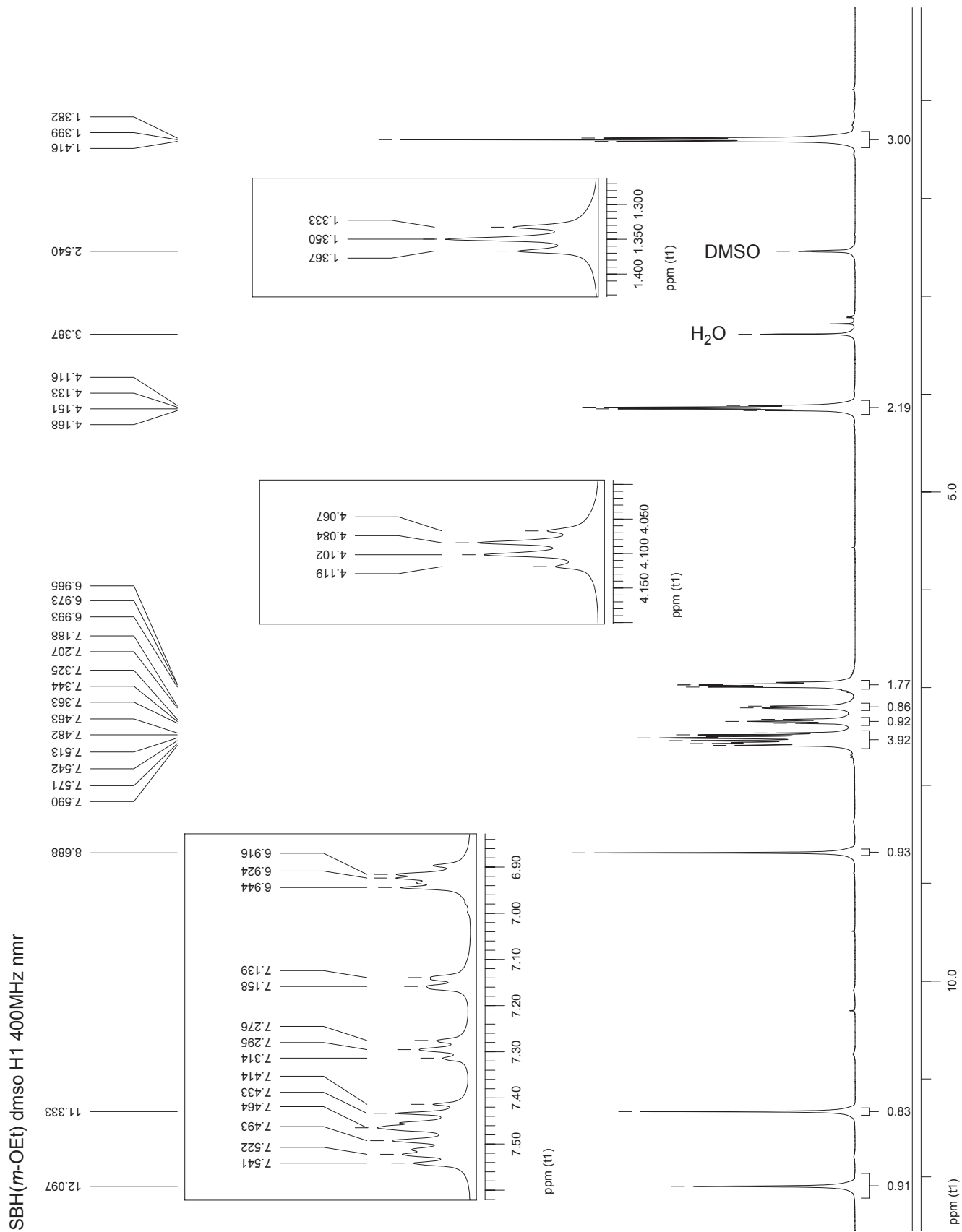


Fig S18. $^1\text{H-NMR}$ spectrum of $\text{BSBH}(\text{OMe})_3$ in deuterated DMSO ($\text{C}_2\text{D}_6\text{SO}$) at 25°C .

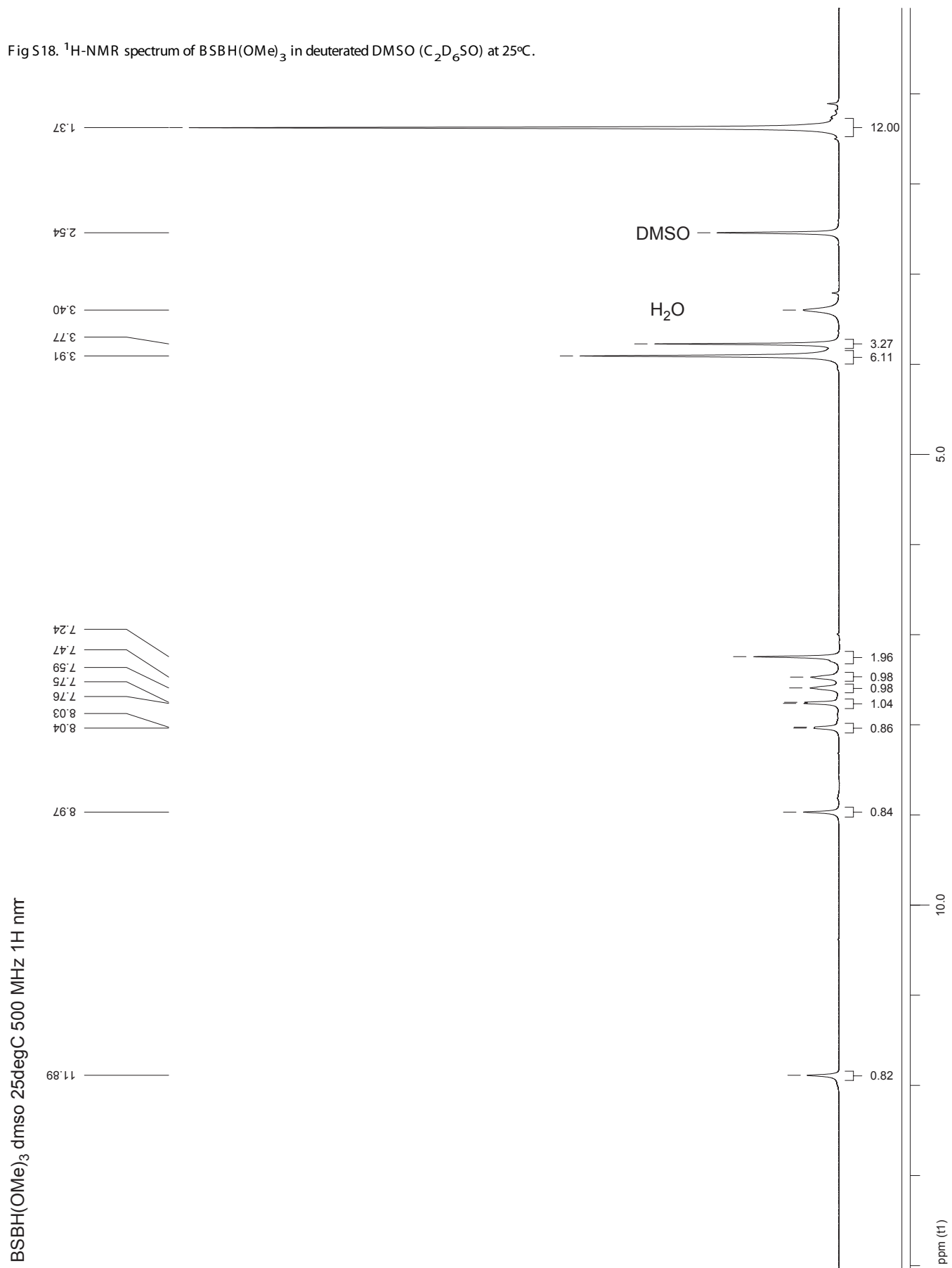


Fig S19. $^1\text{H-NMR}$ spectrum of $\text{SBH}(\text{OMe})_3$ in deuterated DMSO ($\text{C}_2\text{D}_6\text{SO}$) at 25°C .

